© 2016. Published by The Company of Biologists Ltd | Development (2016) 143, 35-44 doi:10.1242/dev.127233

Phosphotyrosyl phosphatase activator facilitates localization of Miranda through dephosphorylation in dividing neuroblasts

Fan Zhang[1,*], Zhen-Xing Huang[2,3,*], Hongcun Bao[1], Fei Cong[1], Huashan Wang[3], Phing Chian Chai[3], Yongmei Xi[4], Wanzhong Ge[4], W. Gregory Somers[5], Ying Yang[3,6], Yu Cai[3,6,‡] and Xiaohang Yang[1,4,‡]

ABSTRACT

The mechanism for the basal targeting of the Miranda (Mira) complex during the asymmetric division of *Drosophila* neuroblasts (NBs) is yet to be fully understood. We have identified conserved Phosphotyrosyl phosphatase activator (PTPA) as a novel mediator for the basal localization of the Mira complex in larval brain NBs. In mutant *Ptpa* NBs, Mira remains cytoplasmic during early mitosis and its basal localization is delayed until anaphase. Detailed analyses indicate that PTPA acts independent of and before aPKC to localize Mira. Mechanistically, our data show that the phosphorylation status of the T591 residue determines the subcellular localization of Mira and that PTPA facilitates the dephosphorylation of T591. Furthermore, PTPA associates with the Protein phosphatase 4 complex to mediate localization of Mira. On the basis of these results, a two-step process for the basal localization of Mira during NB division is revealed: cortical association of Mira mediated by the PTPA-PP4 complex is followed by apical aPKC-mediated basal restriction.

KEY WORDS: *Drosophila* neuroblast, Asymmetric cell division, PTPA, Dephosphorylation of Mira

INTRODUCTION

The asymmetric division of stem cells is a crucial step in development and tissue homeostasis. *Drosophila* neural stem cells or neuroblasts (NBs) have been instrumental for investigating the underlying mechanisms of these fundamental processes (Inaba and Yamashita, 2012; Neumüller and Knoblich, 2009). NBs divide asymmetrically to generate a large apical NB daughter cell and a small differentiating daughter cell, known as the ganglion mother cell (GMC). The former retains a self-renewing capacity, whereas the GMCs have limited proliferation potential. During asymmetric division, cell fate determinants, including the homeobox transcription factor Prospero (Pros) (Doe et al., 1991; Vaessin et al., 1991), the post-transcriptional-repressor Brain tumor (Brat) (Bello et al., 2006; Betschinger et al., 2006; Lee et al., 2006) and the Notch signaling repressor Numb (Rhyu et al., 1994), localize on the basal cortex and are preferentially segregated into the GMCs at telophase. The asymmetric localization of Pros and Brat depends on their common adaptor protein, Mira, whereas the basal localization of Numb is facilitated by its adaptor protein, Partner of Numb (Pon) (Ikeshima-Kataoka et al., 1997; Lee et al., 2006; Lu et al., 1998; Schuldt et al., 1998; Shen et al., 1997).

The precise mechanisms for basal protein localization remain largely elusive. The only mechanistic insight comes from studies of aPKC, a component of the conserved Par complex that also includes Bazooka (Baz) and Par6 (Petronczki and Knoblich, 2001; Schober et al., 1999; Wodarz et al., 2000, 1999). Both Mira and Numb are the substrates of aPKC. Furthermore, aPKC-mediated phosphorylation of Mira is directly inhibited by the action of the tumor suppressor protein Lethal (2) giant larvae [Lgl; L(2)gl – FlyBase] (Atwood and Prehoda, 2009; Wirtz-Peitz et al., 2008).

Several studies have highlighted the importance of protein phosphorylation events in regulating the dynamic assembly of the machinery involved in asymmetric division, as well as in the asymmetric localization of downstream components. The conserved mitotic kinases Aurora A (AurA) and Polo kinase (Polo) have both been identified to act as tumor suppressors in larval NBs by regulating the asymmetric localization of Numb (Lee et al., 2006; Wang et al., 2006, 2007; Wirtz-Peitz et al., 2008). Furthermore, protein dephosphorylation is an important event for localization of basal proteins. Protein phosphatase 2A (PP2A) has been shown to act antagonistically to AurA to suppress aPKC signaling (Chabu and Doe, 2009; Krahn et al., 2009; Ogawa et al., 2009). Larval NBs lacking Falafel (Flfl), a regulatory subunit of Protein phosphatase 4 (PP4), exhibit defective Mira localization whereas localization of Numb remains unaffected. Genetic analyses indicate that Flfl acts in parallel to, or downstream of, Lgl for basal localization of Mira and Pros (Sousa-Nunes et al., 2009).

Phosphotyrosyl phosphatase activator (PTPA) was named based on its *in vitro* ability to stimulate the phosphotyrosyl phosphatase activity of Protein phosphatase 2A (PP2A) (Cayla et al., 1990). Biochemical studies have not only shown that PTPA reactivates the serine/threonine phosphatase activity of inactive PP2A, but also that it increases peptidylprolyl *cis-trans* isomerase activity (Chao et al., 2006). Consistently, the yeast PTPA homologs Ypa1 and Ypa2 can physically bind to the yeast PP2A homologs Pph21 and Pph22. Despite these biochemical findings, the physiological importance of PTPA during development remains unknown.

Here, we report that *Drosophila* PTPA is a regulator for the effective basal localization of the Mira complex during mitosis of larval NB asymmetric divisions. In the absence of PTPA, Mira is cytoplasmic during the early mitotic stage and the basal crescent only becomes evident by anaphase. Our data show that PTPA functions with the PP4 complex to promote the cortical association of Mira, probably through dephosphorylation of the amino acid residue T591, and that this process acts before aPKC. Our results suggest that the basal localization of Mira takes two sequential but independent steps. Dephosphorylation of T591 mediated by PTPA-

[1]College of Life Sciences, Zhejiang University, Hangzhou 310058, China. [2]Institute of Molecular and Cell Biology, ASTAR, 138673 Singapore. [3]Temasek Life Sciences Laboratory, 117604 Singapore. [4]Institute of Genetics, School of Medicine, Zhejiang University, Hangzhou 310058, China. [5]Department of Genetics, La Trobe Institute for Molecular Science (LIMS), La Trobe University, Melbourne, VIC 3083, Australia. [6]Department of Biological Sciences, National University of Singapore, 117543 Singapore.

*These authors contributed equally to this work

‡Authors for correspondence (caiyu@tll.org.sg; xhyang@zju.edu.cn)

Received 27 June 2015; Accepted 9 November 2015

Development (2016) 143, 35-44 doi:10.1242/dev.127233

PP4 is required for timely cortical localization of Mira, which is a prerequisite for the subsequent aPKC-mediated process to restrict Mira to the basal cortex.

RESULTS

Disruption of *Ptpa* specifically affects basal localization of the Mira complex in early mitotic neuroblasts

In an EMS (ethyl methanesulfonate) screen designed to identify genes required for asymmetric division of *Drosophila* larval NBs, we isolated a pupal lethal mutant on the second chromosome that exhibited mislocalized Mira in the type I NBs located in the central brain of larval stage (L) 3. In wild-type (wt) NBs, Mira was localized to the cytoplasm, or mainly to the cytoplasm with a weak basal crescent (collectively referred to as 'non-localized', 92.2%, *n*=90; Fig. 1A,K) during early prophase (defined by scattered condensed chromosomes). Only a small population (7.8%, *n*=90) of NBs exhibited a distinct basal crescent (referred to as 'localized'). In late prophase (when chromosomes had fully condensed and the nuclear membrane had broken down), Mira formed a robust crescent at the basal cortex (74.7%, *n*=91; Fig. 1B,K). Mira continued to be asymmetrically localized during the rest of mitosis (Fig. 1C,D,K) and was preferentially segregated into future GMCs by telophase (Fig. 1E). By contrast, we observed the delayed basal localization of Mira in mutant NBs. In early prophase, all NBs exhibited the cytoplasmic localization of Mira (100%, *n*=51; Fig. 1F,L). In late prophase, Mira distribution remained largely non-localized in the majority of mutant NBs (88.9%, *n*=117; Fig. 1G,L). However, defective cortical localization of Mira was partially recovered by metaphase and about half of NBs (56.4%, *n*=55; Fig. 1H,L) exhibited a cytoplasmic localization of Mira. By anaphase, although the majority of NBs displayed basal Mira crescents (93.3%, *n*=15; Fig. 1I,L), some NBs (6.7%, *n*=15) still exhibited cytoplasmic localization of Mira (Fig. 1L). By telophase, Mira was preferentially segregated into the GMCs (Fig. 1J).

Complementation-based deficiency mapping of this EMS mutation identified a lethal region uncovered by *Df(2L)BSC164*, but not *Df(2L)BSC163*. Together, this defined a genomic region with seven candidate genes (Fig. 1M). A genomic fragment within this candidate region (*BAC CH322-119I09*) was tested and was shown to rescue both the lethality and Mira localization defects when introduced in this mutant background. This further refined the candidate to a single conserved gene, *Phosphotyrosyl phosphatase activator* (*Ptpa*) (Fig. 1M). Sequence analysis of this EMS mutant line revealed a C to T mutation within the coding sequence, resulting in a premature stop codon at position 126 in the PTPA amino acid sequence. Both *Ptpa* homozygous and the *Ptpa/Df(2L)BSC164* hemizygous animals survived to the pupal stage and displayed NB phenotypes to similar severities (data not shown). This suggests that the mutant is a functional null allele. Furthermore, expression of full-length *Ptpa* cDNA, driven by *wor-gal4*, was able to rescue Mira localization defects in mutant NBs (Fig. 2F,G). This confirmed that the observed defective localization of Mira was due to a disruption in the *Ptpa* gene. We named the mutant $Ptpa^{1}$. Subsequent analyses in this study were carried out with this allele.

To gain a better insight into the dynamic localization of Mira in the $Ptpa^{1}$ mutant background, we utilized a functional GFP-tagged Mira transgene and conducted time-lapse imaging analyses (Fig. 1N-U) (Erben et al., 2008). Consistent with our observation in fixed tissues, Mira-GFP exhibited a basal localization in wt NBs during prophase and metaphase (Fig. 1N-Q, Movie 1) whereas mutant NBs showed a mainly cytoplasm localization (Fig. 1R-U). Although live imaging showed an extended prophase in the mutant NBs, the length of time between metaphase and the end of mitosis was similar to that of the wt (Movie 2). Mutant NBs segregated Mira into the GMCs upon the completion of mitosis, as did their wt counterparts. Based on these observations, we conclude that the formation of robust basal Mira crescents is delayed in the majority of mutant NBs.

We then investigated the localization of other components involved in NB asymmetric division in the $Ptpa^{1}$ mutant background. As expected, both Pros and Brat colocalized with Mira in the cytoplasm during early mitotic stages (Fig. S1A-H). Interestingly, the basal localization of the Pon-Numb complex remained unaffected (Fig. S1E-H). All apical components, including aPKC, Inscuteable (Insc) and Pins (Partner of Inscuteable) (Kraut et al., 1996; Wodarz et al., 2000; Yu et al., 2000), localized normally in dividing NBs (Fig. 1G-J, Fig. S1A-D; data not shown). Based on these results, we conclude that PTPA functions specifically to facilitate the basal localization of the Mira complex in early mitotic NBs.

PTPA encodes a nuclear protein

To determine the expression pattern and subcellular localization of PTPA, we generated a polyclonal antibody against full-length PTPA. As had been predicted, western blot analysis showed that this antibody recognized a strong band with a molecular mass of approximately 45 kDa in wt L3 brain extracts. This band was not detected in brain extracts from the $Ptpa^{1}$ mutant (Fig. 2A). In addition, immunofluorescent staining with the antibody revealed general PTPA expression in many cells, including all NBs in the L3 brain. PTPA was enriched in the nuclei during interphase and became dispersed evenly throughout the cytoplasm after breakdown of the nuclear envelope (Fig. 2B,C). The anti-PTPA antibody failed to detect any specific signal in the $Ptpa^{1}$ mutant NBs (Fig. 2D). This confirmed its specificity to PTPA. A similar subcellular localization was observed when the PTPA transgene was expressed in NBs of the wt (Fig. 2E) or $Ptpa^{1}$ mutant larval brains (Fig. 2F,G), in which the overexpressed PTPA rescued the Mira localization defects.

PTPA facilitates dephosphorylation of Mira T591

Previous studies have indicated that the dynamic subcellular localization of Mira depends on its phosphorylation status (Sousa-Nunes et al., 2009; Sousa-Nunes and Somers, 2010). This prompted us to investigate whether Mira mislocalization in $Ptpa^{1}$ mutants was a reflection of its inappropriate phosphorylation status. To address this issue, we performed two-dimensional (2D) western blotting to directly assess the phosphorylation status of Mira in wt and $Ptpa^{1}$ mutant brain extracts.

As revealed by 2D western blotting analysis, Mira indeed exhibited various phospho-isoforms in the wt brain extracts (Fig. 3A). This probably corresponds to the different subcellular localization stages in the NBs at various cell cycle phases. Hyper-phosphorylated Mira, with a lower isoelectric point migrates more towards the acidic (+) end, whereas hypo-phosphorylated Mira moves towards the basic (−) end (Fellner et al., 2003). As expected, the $Ptpa^{1}$ mutant brain extracts exhibited a shift towards the acidic (+) end, indicating a higher proportion of hyper-phosphorylated Mira, compared with those of the wt samples (Fig. 3A). These results are consistent with the notion that PTPA, as a phosphatase activator, acts in the dephosphorylation process of Mira and that the loss of PTPA function results in the accumulation of hyper-phosphorylated Mira.

Development (2016) 143, 35-44 doi:10.1242/dev.127233

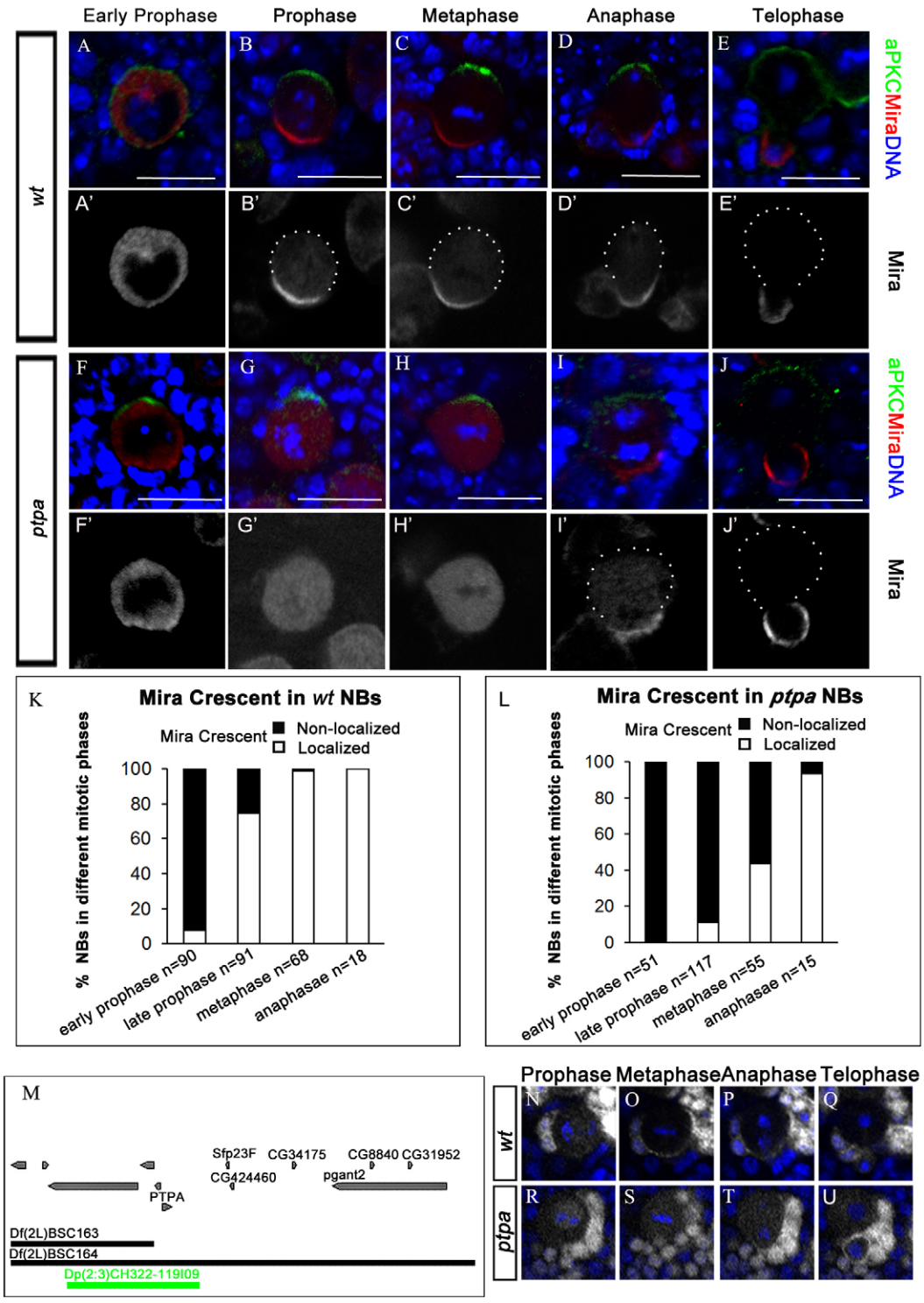

Fig. 1. Disruption of *Ptpa* causes delay of basal localization of the Mira complex. (A-J′) wt (A-E′) and *Ptpa*^{1} (F-J′) L3 larval brain NBs stained for aPKC (green), Mira (red) and DNA (blue) in various cell cycle phases. NBs in B-E and I,J are outlined with white dots in B′-E′,I′,J′. (K,L) Quantification of crescent-localized and non-localized Mira in different mitotic phases of wt and *Ptpa*^{1} NBs. (M) Schematic representation of *Ptpa* locus and deletion mapping of *Ptpa*^{1} mutant. The deleted region of the deficiency stock is shown as a black line and the duplicated region for generating transgenic rescue line is shown as a green line. (N-U) Still frames from time-lapsed imaging of Mira localization in L3 larval NBs, showing Mira's sequential location (grey) for a single cell cycle in wt (N-Q) and *Ptpa*^{1} mutant NBs (R-U). DNA is visualized with Histone::mRFP (blue). Scale bars: 10 µm.

It has previously been shown that S2 cells are able to faithfully replicate the cytoplasmic and cortical localization of Mira detected in NBs (Atwood and Prehoda, 2009). We next investigated whether the shift in Mira phosphorylation status could be replicated upon *Ptpa* knockdown in S2 cells. A *3HA::mira* construct was transiently introduced into S2 cells with or without *Ptpa* dsRNA treatment (Fig. S2A). Mira was pulled down using an anti-HA antibody and subjected to 2D western blotting analysis. The *Ptpa* RNAi samples

Development (2016) 143, 35-44 doi:10.1242/dev.127233

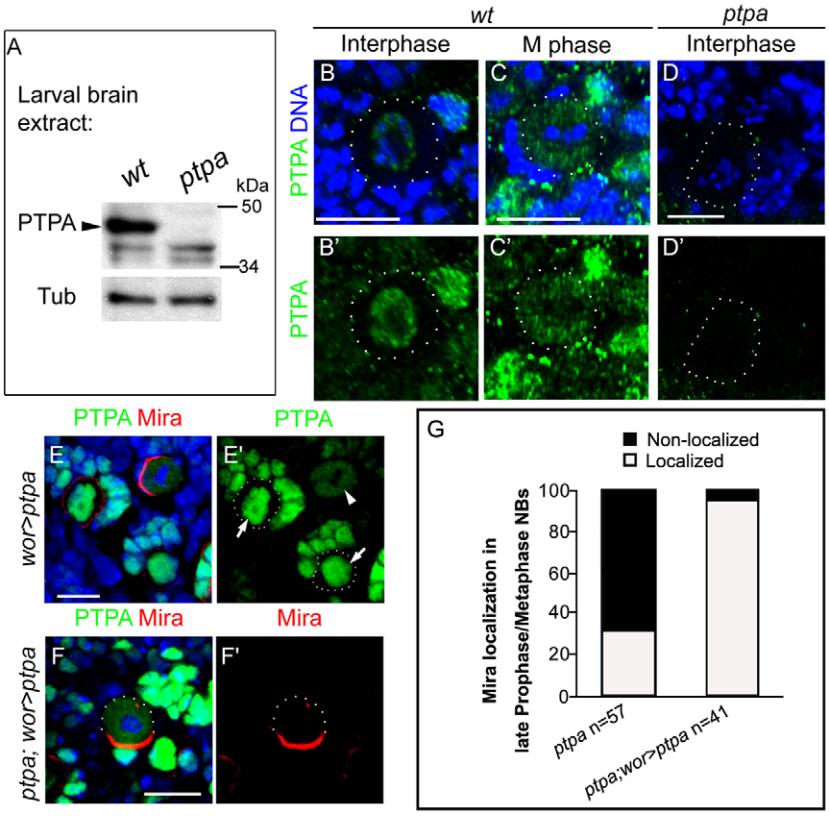

Fig. 2. *Ptpa* encodes a nuclear protein. (A) The anti-PTPA antibody recognizes a specific band (arrowhead) in the wt but not in *Ptpa*^{1} mutant brain lysate. (B-C′) wt larval brain stained with anti-PTPA. In NBs, PTPA (green) mainly localizes to the nucleus during interphase and throughout cytoplasm in metaphase (M phase). (D,D′) No specific signal is detected in *Ptpa*^{1} NBs. (E-F′) The exogenous PTPA recapitulates the endogenous subcellular localization (E,E′) and rescues Mira localization defects (F,F′). NBs are outlined with white dots. Arrows indicate interphase NBs; arrowhead indicates mitotic NB. (G) Quantification of Mira localization in the *Ptpa*^{1} mutant NBs rescued with *Ptpa* transgene. Scale bars: 10 µm.

consistently reproduced a shift in Mira towards the acidic end compared with that of the controls (Fig. 3B,C). This observation was similar to that in the *Ptpa*^{1} mutant total brain extracts (Fig. 3A). In addition, we noticed one unique signal spot that was present only in the *Ptpa* RNAi sample (solid arrow, Fig. 3C), but not in the control (open arrow, Fig. 3B). This suggests that the signal spot reflects the transient phosphorylation status of Mira as regulated by PTPA activity.

We then pursued the identity of the putative Mira phosphorylation site(s) modulated by PTPA. Ectopically expressed 3HA::Mira was immunoprecipitated with anti-HA antibodies from S2 cells and subjected to mass spectrometry analysis. This showed that the T591 residue of Mira was hyper-phosphorylated in *Ptpa* RNAi samples, but not in the controls (Table S1). To address whether the phosphorylation status of this site was indeed linked to PTPA function, we mutated T591 to alanine to mimic a non-phosphorylated form and then re-examined the migratory pattern of this Mira variant (Mira^{T591A}). In 2D western blotting analysis, the unique signal spot observed in the S2 samples treated with *Ptpa* dsRNA (solid arrow, Fig. 3C) was not detected in the cell extracts with overexpressed Mira^{T591A} (open arrow, Fig. 3D). This unique signal spot probably represents the population of Mira with phosphorylated T591. Conversely, when the T591 residue was mutated to aspartic acid (T591D), to mimic the phosphorylated form of Mira (referred to as Mira^{T591D}), the unique signal spot remained observable in the S2 cell extracts (solid arrow, Fig. 3E). On the basis of these findings, we conclude that the unique signal spot, as detected in the analysis of S2 samples treated with *Ptpa* dsRNA, is specifically linked to Mira molecules with phosphorylated T591 and suggest that this phosphorylation is regulated by PTPA activity. Thus, PTPA is likely to function to facilitate the dephosphorylation of T591 of Mira. In the absence of PTPA, dephosphorylation is impaired and Mira remains hyper-phosphorylated.

Phosphorylation status of T591 determines Mira localization

To further explore the relationship between T591 phosphorylation status and Mira localization, we addressed the potential role of PTPA on Mira localization in S2 cells. As reported previously, overexpressed Mira was detected both in the cytoplasm and on the cortex of untreated cells (Fig. 3G, Fig. S2B). However, knockdown of *Ptpa* led to a significant increase of cytoplasmic Mira (Fig. 3H, Fig. S2B). As expected, Mira^{T591D} in S2 cells was predominantly cytoplasmic (Fig. 3I, Fig. S2B), recapitulating the Mira mislocalization phenotype observed in *Ptpa* RNAi cells and in *Ptpa*^{1} NBs. By contrast, nonphosphorylatable Mira^{T591A} was found primarily on the cell cortex (Fig. 3J, Fig. S2B).

These data provide strong evidence supporting the hypothesis that the phosphorylation status of the T591 residue is closely linked to Mira localization in S2 cells. Phosphorylated T591 Mira molecules remain primarily in the cytoplasm, whereas unphosphorylated T591 molecules are enriched on the cell cortex. PTPA probably facilitates the dephosphorylation of T591. This, in turn, regulates the cortical localization of Mira. To test this hypothesis *in vivo*, we generated transgenic flies carrying these Mira variants and examined the subcellular localization of these variants in dividing NBs upon overexpression. Anti-Mira antibodies showed that the majority of late prophase NBs expressing Mira^{T591D} exhibited cytoplasmic Mira staining (64.9%, *n*=97; Fig. 3L, Fig. S2C), in a manner reminiscent of Mira localization in the *Ptpa*^{1} mutant (88.9%, *n*=117; Fig. 1L). In addition, a high percentage (37.4%, *n*=91) of metaphase NBs expressing Mira^{T591D} exhibited cytoplasmic Mira staining (Fig. 3O, Fig. S2C). This was consistent with the Mira localization defects observed in *Ptpa* mutant (56.4%, *n*=55; Fig. 1L). By contrast, Mira was predominantly localized to the basal cortex in NBs expressing the Mira^{T591A} protein, both in prophase (67%, *n*=91; Fig. 3M, Fig. S2C) and metaphase (97.3%,

Development (2016) 143, 35-44 doi:10.1242/dev.127233

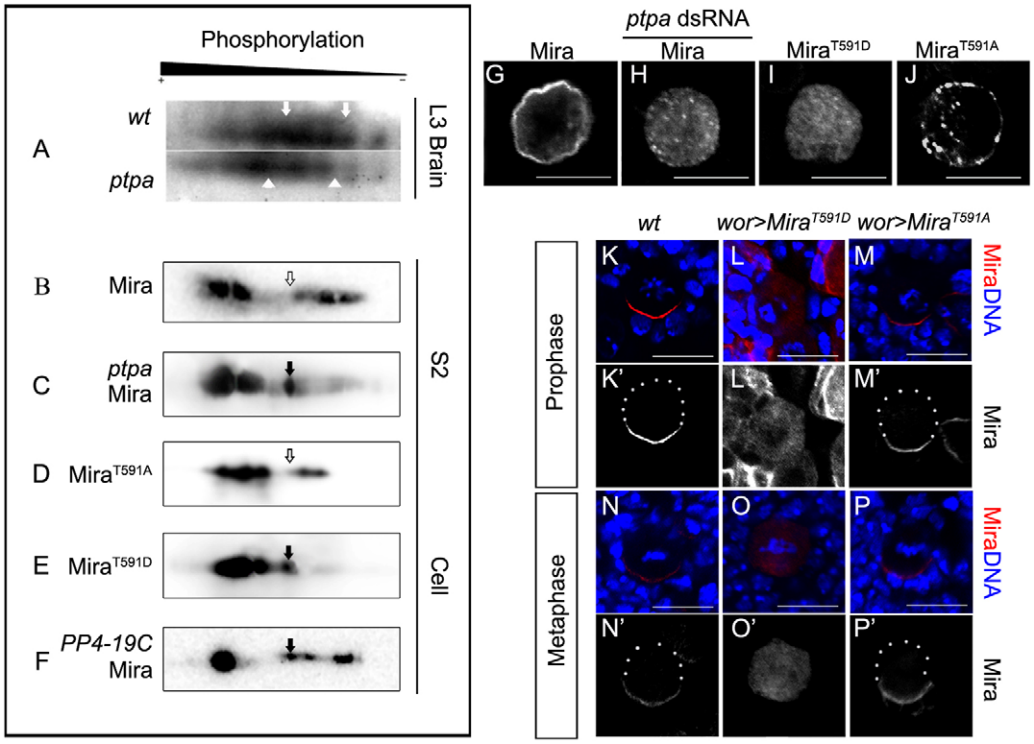

Fig. 3. PTPA facilitates Mira dephosphorylation. (A) 2D western blot of L3 larval brain lysates from *wor>mira::3GFP* in wt and *Ptpa*^{1} mutant background probed with anti-GFP antibody. The overall Mira phosphor-isoforms shift towards the acidic ends in *Ptpa* mutant samples compared with those of the control samples. (B-F) 2D western blots of S2 cell lysates from overexpression of *3HA::mira* and *mira* variants in various backgrounds and detected with anti-HA. One unique signal spot is detected in the S2 sample treated with *Ptpa* dsRNA (C, solid arrow) but not in the S2 sample alone (B, open arrow). The identical signal spot is also detected in the S2 sample transfected with phosphor-mimic variant (E, Mira^{T591D}, solid arrow) but not non-phosphorylatable variant (D, Mira^{T591A}, open arrow). This signal spot is also detected in S2 sample treated with *PP4-19C* dsRNA (F, solid arrow). (G-J) Localization of Mira and its variants in S2 cells. Mira is both on the cortex and in the cytoplasm in S2 cells (G). Upon *Ptpa* dsRNA treatment, Mira is located mainly in the cytoplasm in S2 cells (H). The Mira^{T591D} variants exhibit cytoplasmic localization (I), whereas Mira^{T591A} is largely associated to the cortex (J). (K-P′) Localization of Mira and its variants in larval NBs. During prophase and metaphase, Mira forms a basal crescent in wt (*wor-gal4*/+) NBs (K,K′,N,N′). Mira is detected in the cytoplasm in NBs expressing Mira^{T591D} of same mitotic stages (L,L′,O,O′), whereas expression of Mira^{T591A} has no effect on Mira localization (M,M′,P,P′). Scale bars: 10 µm.

n=74; Fig. 3P, Fig. S2C), in a manner reminiscent of the endogenous Mira localization in wt NBs (Fig. 3K,N, Fig. S2D).

Taken together, these results strongly suggest that the phosphorylation status of T591 plays an essential role in Mira subcellular localization during early stages of mitosis. During prophase, Mira with phosphorylated T591 exhibits a cytoplasmic localization, whereas Mira molecules with dephosphorylated T591 are enriched on the cell cortex.

PTPA-mediated cortical localization of Mira precedes aPKC function

It has been shown that aPKC-mediated phosphorylation of Mira at five sites (96S, 194T, 195S, 205T and 206S; collectively referred to as the aPKC sites) is necessary and sufficient to displace Mira from the cell cortex into the cytoplasm (Atwood and Prehoda, 2009). In order to understand whether defective localization of Mira in the *Ptpa*^{1} mutant was caused by upregulated aPKC activity on the cortex, we explored the epistatic relationship between PTPA and aPKC in establishing the cortical localization of Mira during NB division. Here, we took advantage of a Mira variant that is non-phosphorylatable by aPKC (Mira5A, where all five aPKC sites are mutated to alanine), as well as a mutated form of the cytoskeletal protein Lgl (Lgl3A), the ectopic expression of which leads to defective localization of Mira that is similar to that of the aPKC loss-of-function mutant (Betschinger et al., 2003).

As previously reported, when ectopically expressed in wt NBs, Mira5A localized to the entire cell cortex (93.5%, *n*=31; Fig. 4A,C). However, in *Ptpa*^{1} mutant NBs, Mira5A remained cytoplasmic in the majority of prophase/metaphase NBs (58.3%, *n*=41; Fig. 4B,C). This was similar to the observations of endogenous Mira in *Ptpa*^{1} mutant NBs (Fig. 1H,L). These results indicate that the failure of cortical localization of Mira in the *Ptpa*^{1} mutant is independent of aPKC activity on the cortex. It also further suggests that the cortical association of Mira precedes its basal localization.

To confirm the notion that PTPA-dependent cortical localization of Mira acts before aPKC, we attenuated aPKC function toward Mira by ectopic expression of the Lgl3A transgene. As expected, when ectopically expressed in wt NBs, Lgl3A localized to the entire cell cortex. This resulted in the even distribution of Mira around the cell cortex (Fig. 4D,H). By contrast, although Lgl3A localized to the entire cell cortex in *Ptpa*^{1} mutant NBs, Mira remained in the cytoplasm of NBs (72.1%, *n*=43; Fig. 4E,H). These results strengthen the notion that failure of the cortical association of Mira is not due to aPKC activity on the cortex. We further substantiated this result by knocking down aPKC in *Ptpa*^{1} mutant NBs using an inducible *aPKC* RNAi transgene. Attenuating aPKC to levels below detection by immunofluorescence resulted in an even distribution of Mira around the entire cortex (Fig. 4F,H) in the majority of wt NBs. However, in the *Ptpa*^{1} mutant, Mira remained in the cytoplasm in

Development (2016) 143, 35-44 doi:10.1242/dev.127233

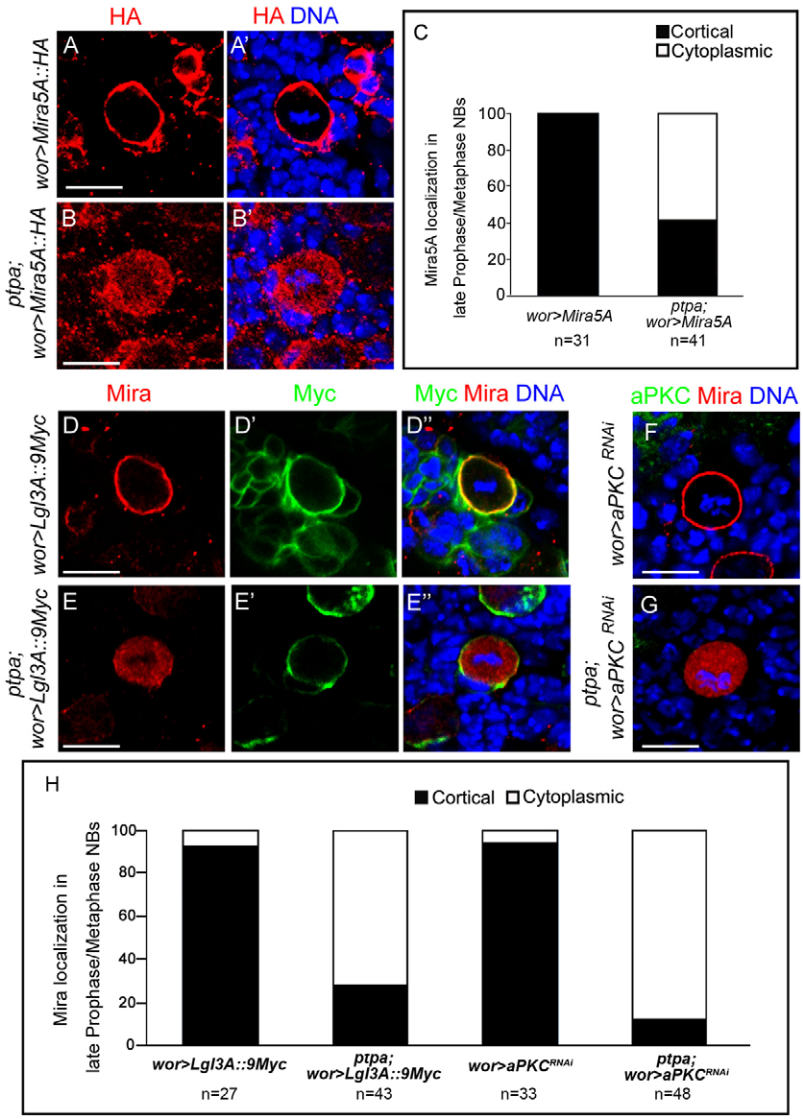

Fig. 4. PTPA mediates Mira cortical localization independent of aPKC activity. (A-B′) Mira5A (*HA::mira5A*, non-phosphorylatable by aPKC) is cortically localized in wt NBs (A,A′) but remains in the cytosol in the *Ptpa*^{1} mutant NB (B,B′). (C) Quantification of *HA::mira5A* localization in late prophase/metaphase of wt versus *Ptpa*^{1} NBs. (D-E″) Endogenous Mira exhibits cortical localization in wt metaphase NBs expressing Lgl3A::9Myc (D-D″) but is cytoplasmic in *Ptpa*^{1} NBs expressing Lgl3A::9Myc (E-E″). (F,G) Endogenous Mira localizes to the entire cortex in wt L3 NBs expressing *aPKC* dsRNA (F) but remains in the cytoplasm in *Ptpa*^{1} NBs expressing *aPKC* dsRNA (G). (H) Quantification of Mira localization phenotype in wt and *Ptpa*^{1} NBs with attenuation of aPKC activity. Scale bars: 10 µm.

87.5% (*n*=48) of pro/metaphase NBs (Fig. 4G,H). This is consistent with early observations in NBs overexpressing Lgl3A.

In summary, these results provide strong evidence that PTPA-mediated cortical localization of Mira during early mitotic stages is not related to the phosphorylation of Mira on the five aPKC sites. It also confirms that the mislocalization of Mira in *Ptpa*^{1} NBs is not due to excessive aPKC activity on the cell cortex. Instead, these data suggest that PTPA-mediated cortical localization of Mira precedes aPKC-mediated basal localization. Thus, we propose that the asymmetric localization of Mira during mitosis takes two sequential but independent steps. Firstly, PTPA-mediated dephosphorylation of T591 is required for efficient and timely Mira cortical translocation. This acts before the apical aPKC activity that then restricts Mira to the basal cortex.

PTPA interacts with PP4 to regulate Mira localization

Our data show that the PTPA-mediated dephosphorylation of the T591 residue is the major factor for cortical localization during early mitosis. We next addressed the underlying mechanism of PTPA function. It has been previously reported that yeast PTPA homologs not only bind to PP2A, but also interact with other PP2A-like family members, including PP4, *in vitro* (Van Hoof et al., 2005).We then investigated whether PTPA interacts with either of the PP2A or PP4 protein phosphatase complexes to regulate Mira localization.

In contrast to our observations that disruption of PTPA function in early mitosis affects localization of the Mira complex in a manner independent of aPKC, PP2A has been shown to regulate the basal localization of both the Mira and Numb complexes by antagonizing aPKC activity (Chabu and Doe, 2009; Ogawa et al., 2009; Wang et al., 2009). To investigate whether there was a correlation between PP2A activity and PTPA-mediated Mira localization during mitosis, we manipulated Mts (the catalytic subunit of PP2A) levels in the *Ptpa*^{1} mutant background. Neither ectopic expression of Mts nor the removal of one copy of the *mts* gene influenced the Mira localization defects in the *Ptpa*^{1} mutant (Fig. S3). These observations suggest that Mts, and presumably the PP2A complex, is not involved in the PTPA-mediated Mira localization pathway.

Flfl, the regulatory subunit of the serine/threonine-specific PP4 complex, has been reported to regulate localization of the Mira complex through a pathway acting downstream of, or in parallel to, the aPKC-Lgl pathway (Sousa-Nunes et al., 2009). This prompted us to examine the potential relationship between PTPA and the PP4 complex. We first examined whether PTPA colocalized with

Development (2016) 143, 35-44 doi:10.1242/dev.127233

subunits of the PP4 complex in NBs. PP4-19C, the catalytic subunit of the *Drosophila* PP4 complex, localized predominantly to the cytoplasm during interphase and exhibited a transient nuclear enrichment during early prophase. This was followed by cytoplasmic localization after the breakdown of the nuclear envelope (Fig. 5A-C). PTPA colocalized with PP4-19C in the cytoplasm in mitotic NBs. Further study revealed that Flfl exhibited a similar localization pattern to PTPA during mitosis (Fig. S4A,B). These results suggest that PTPA has the potential to form a complex with PP4-19C. To test this possibility, we performed co-immunoprecipitation experiments and found that endogenous PTPA was pulled down by an anti-PP4-19C antibody from S2 cell lysates (Fig. 5D). This suggests that *in vivo*, PTPA probably forms a protein complex with PP4.

We then examined PP4-19C expression using western blotting and found that PP4-19C protein levels were upregulated in the *Ptpa*^{1} mutant brain samples (Fig. 5E). This upregulation occurred at the post-transcriptional level (Fig. S4C). Furthermore, mosaic analysis with a repressible cell marker (MARCM), also confirmed that PP4-19C was upregulated in *Ptpa*^{1} NBs (Fig. 5F). These data indicate that PTPA regulates PP4-19C expression levels. To explore the possibility that PTPA functions through the PP4 pathway to regulate Mira localization, we performed genetic interactions between *Ptpa*^{1} and the PP4 complex. Indeed, the frequency of NBs exhibiting cytoplasmic Mira at prophase or metaphase increased from 68.4% (n=57; Fig. 5G) in the *Ptpa*^{1} mutant to 86.9% (n=76; Fig. 5G) when one copy of the *flfl* gene was removed from the *Ptpa*^{1} background. This suggested an interaction between PTPA and the PP4 complex. To gain further support, we used an RNAi transgene that effectively knocked down PP4-19C expression levels in the *Ptpa*^{1} mutant (Fig. S4D,E). Knockdown of PP4-19C markedly enhanced Mira localization defects in almost all of the *Ptpa*^{1} NBs that exhibited cytoplasmic Mira in early mitotic stages (98.9%, n=95; Fig. 5G).

These results strongly suggest that PTPA and PP4 function along the same genetic pathway to regulate Mira localization during early mitosis. To address whether the PP4 complex is involved in regulating T591 phosphorylation in the same manner as PTPA, we performed 2D western blot analysis on S2 cell extracts treated with *PP4-19C* dsRNA. The uniquely phosphorylated T591 signal spot, observed in *Ptpa*^{1} RNAi samples, was also detected in PP4-19C-knockdown cell extracts (solid arrow, Fig. 3F). This supports the notion that the PTPA and PP4 complexes act together to facilitate the dephosphorylation of T591 of Mira.

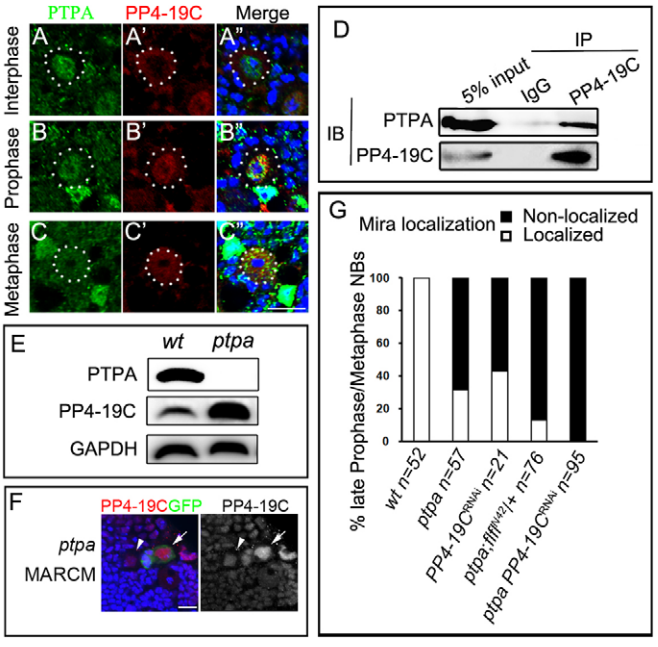

Fig. 5. PTPA interacts with PP4 in the same genetic pathway. (A-C″) In wt NBs, PP4-19C (red) is localized to the nucleus and cytoplasm in interphase and prophase (A-B″), whereas PTPA (green) is predominantly in the nucleus (A-B″). At metaphase, both PP4-19C and PTPA localize throughout the cytoplasm (C-C″). (D) Endogenous PTPA is pulled down by anti-PP4-19C antibody from S2 cells. (E) PP4-19C is upregulated in *Ptpa*^{1} mutant brains. (F) A MARCM clone of *Ptpa*^{1} NB showing that PP4-19C protein level is upregulated (arrow) compared with wt NB (arrowhead). (G) Quantification of Mira localization in various genetic backgrounds. Scale bars: 10 µm.

DISCUSSION

Proper localization of the Numb and Mira complexes has been proposed to involve the translocation of these proteins to the cell cortex, followed by an aPKC-mediated process that restricts their enrichment to the basal cortex (Atwood and Prehoda, 2009; Smith et al., 2007). Despite studies showing that Numb and Mira behave similarly in dividing NBs, each complex has its unique basal targeting machinery. In this study, we identify PTPA as a specific player that mediates the basal localization of the Mira complex during NB divisions. We further elucidate the mechanism by which PTPA regulates cortical localization of Mira, which occurs during early mitosis, before the aPKC-mediated basal restriction process.

Phosphorylation status of T591 determines Mira localization in early mitosis

In the majority of *Ptpa*^{1} NBs, the formation of the Mira crescent is delayed and Mira mislocalizes during early mitotic stages. This defect is largely recovered by anaphase, allowing the appropriate segregation of Mira and its cargoes into GMC daughters at telophase. Results from both *in vitro* and *in vivo* experiments support our hypothesis that dephosphorylation of the T591 residue of Mira is controlled by PTPA-mediated activity and that the phosphorylation status of Mira T591 determines its subcellular localization. The 2D western blot data reveal a unique signal spot corresponding to Mira molecules with phosphorylated T591. This spot was detected only in extracts from *Ptpa* knockdown and phosphorylation-mimetic Mira^{T591D}-expressing cells, but not from wt and non-phosphorylatable Mira^{T591A} samples. We further established the link between Mira cortical localization and the phosphorylation status of T591 using two Mira variants. Phospho-mimetic Mira^{T591D} predominantly localizes in the cytoplasm of both the S2 cells and the L3 brain NBs whilst non-phosphorylatable Mira^{T591A} is enriched on the cell cortex. Thus, our data unveil the mechanism for Mira translocation from cytoplasm to cortex during early mitosis. It also suggests that the dephosphorylation of T591 (which primes the cortical association of Mira) is an important step for its asymmetric localization.

Interestingly, we found that Mira is largely cytoplasmic in NBs expressing the Mira^{T591D} variant. This suggests that Mira^{T591D} behaves as a dominant-negative form. It is interesting that the T591 residue falls in the cargo-binding domain (460-660 aa) of the Mira molecule, which also participates in dimer formation (Fuerstenberg et al., 1998; Matsuzaki et al., 1998; Shen et al., 1998; Yousef et al., 2008). One possible explanation for the dominant-negative effect of Mira^{T591D} is that the phosphorylation status of T591 does not affect Mira dimerization. Mira^{T591D}, when expressed in wt NBs, is able to form a heterodimer with endogenous Mira. Dephosphorylation of

Development (2016) 143, 35-44 doi:10.1242/dev.127233

T591 in both Mira molecules needs to occur to allow effective cortical association of the dimerized Mira.

PTPA-mediated Mira cortical localization is independent of and acts before aPKC

It has been reported that Mira basal localization requires aPKC activity that phosphorylates Mira on five aPKC sites (Atwood and Prehoda, 2009). In this study, we have identified a new phosphorylatable site, T591, dephosphorylation of which is mediated by PTPA-PP4. In addition, because only the cortex-bound form of aPKC is active and PTPA-mediated dephosphorylation of T591 drives Mira from the cytoplasm to the cortex upon mitosis, the physiological function of PTPA in the NBs is likely to provide a substrate for aPKC on the cell cortex in a timely manner during NB division. This timely localization of Mira and its cargo is probably important in the maintenance of NB self-renewal. This is supported by the observation of a moderate decrease in NB number at late third instar larval stage (our unpublished data). However, *Ptpa*^{1} mutant NBs also preferentially segregate the Mira complex into the GMC daughters upon completion of division, as in wt NBs. Consistent with this, using time-lapsed imaging of wt NBs, we observed a decrease in the cytosolic pool of Mira before its basal enrichment (Movie 1). However, the clearance of cytoplasmic Mira and its basal enrichment was delayed in the *Ptpa*^{1} mutant NBs (Movie 2). This is in line with the role of PTPA for the effective cortical localization of Mira. We further exclude the possibility that defective Mira localization in the *Ptpa*^{1} mutant is due to an excess of aPKC activity and show that attenuation of aPKC activity towards Mira, by expressing Lgl3A or dsRNA against *aPKC* in the *Ptpa*^{1} mutant, does not rescue the defective Mira localization phenotype. These observations also imply that aPKC is not responsible for the phosphorylation of T591 and we predict the existence of one yet-to-be-identified kinase that acts in early in mitosis to phosphorylate the T591 residue before the action of PTPA-PP4. We conclude that PTPA-mediated dephosphorylation of T591 is independent of and occurs before aPKC activity.

PTPA acts with PP4 to control cortical localization of Mira

Our data show that PTPA facilitates the dephosphorylation of T591 during prophase. As PTPA itself lacks phosphatase activity, it must participate in a phosphatase complex to perform dephosphorylation. It was reported that PTPA functions as an activator of PP2A *in vitro*. However, our data failed to ratify the involvement of the PP2A complex in the *Ptpa*^{1} mutant phenotype. By contrast, removing one copy of *flfl*, or knockdown of PP4-19C in *Ptpa*^{1} mutants, exaggerates defects in Mira localization. These observations suggest that PP4-19C may share the same genetic pathway as PTPA. This is supported by results showing that endogenous PTPA forms a complex with PP4-19C during mitosis. More importantly, the unique signal spot corresponding to phosphorylated T591 population of Mira is also detected in 2D western blot when PP4 activity is reduced. Our findings therefore suggest that PTPA binds the catalytic subunit of PP4 and acts along the same genetic pathway as that controlling the dephosphorylation of T591. It would be interesting to determine whether T591 is a direct target of the PTPA-PP4 complex. In this scenario, PTPA-PP4 is able to mediate the efficient dephosphorylation of T591 during prophase, thus providing Mira on the cortex for subsequent aPKC-mediated basal enrichment. In the absence of PTPA, PP4 activity is compromised and, by an unknown mechanism, NBs then upregulate PP4-19C to compensate for the reduction in PP4 activity. As a result, PP4-mediated dephosphorylation of T591 is inefficient and the cortical localization of Mira is delayed.

In summary, our study reveals the physiological function of PTPA in two distinct but sequential steps for Mira localization during early mitosis in *Drosophila* NBs (Fig. 6). PTPA, together with PP4, first mediates the dephosphorylation of T591 residues. This, in turn, drives Mira from the cytoplasm to the cell cortex where the apically enriched aPKC restricts Mira localization to the basal cortex.

MATERIALS AND METHODS

Fly strains

The *Ptpa*^{1} mutant was identified from the phenotypic analysis of an EMS screen using standard protocol (W.G.S. and W. Chia, unpublished results). The following fly stocks were used in this study: *wor-gal4*, Df(2L)BSC163, Df(2L)BSC164, Df(2R)BSC359, *mts*$^{XE-2258}$, *His2av::mRFP*, *PP4-19C*^{RNAi} (V25317), *aPKC*^{RNAi} (KK10087) (Vienna *Drosophila* RNAi Center), BAC CH322-119I09 (from Exelixis at Harvard Medical School), *UAS-Dicer2*, *flfl*^{N42} (Sousa-Nunes et al., 2009), *UAS-HA::mira5A* (Atwood and Prehoda, 2009), *UAS-Lgl3A::Myc* (Betschinger et al., 2003), *UAS-mira::3GFP* (gift from C. Petritsch, UCSF). MACRM clones were generated as previously described (Chai et al., 2013). For GFP-labeled *Ptpa*^{1} mutant clones, we used an *elav-gal4,hs-FLP;UAS-nlacZ,UAS-mCD8::GFP;P[FRT]40A,*

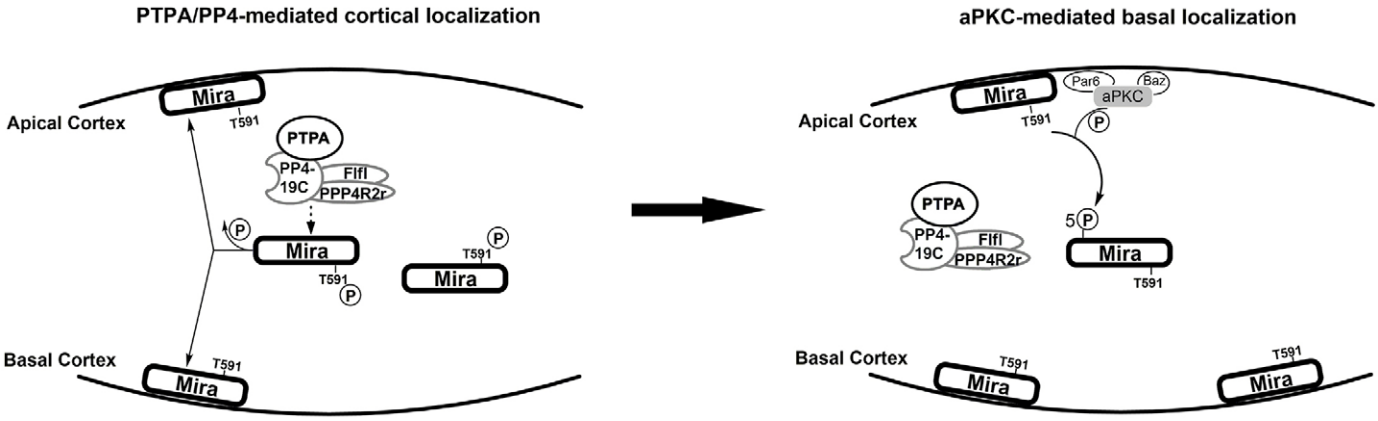

Fig. 6. Diagram depicting two sequential steps for Mira localization in *Drosophila* mitotic NBs. (Left) During early mitosis, Mira localizes to cytosol and is phosphorylated at T591. After the nuclear membrane breaks down, PTPA, together with the PP4 complex, facilitates dephosphorylation of the T591 residue, which leads to the cortical association of Mira. (Right) In the cortex, the apically localized aPKC complex will then phosphorylate Mira on those five aPKC sites, which displaces Mira from the apical cortex. This results in the basal restriction of Mira.

Development (2016) 143, 35-44 doi:10.1242/dev.127233

tubP-GAL80 driver (Bello et al., 2006). For *PP4-19C*RNAi knockdown clones, the fly line with the genotype of *hs-FLP1.22*; *act-y*$^{+}$*-gal4*; *UAS-GFP*/PP4-19C^{RNAi} was used. GFP-labeled *PP4-19C*^{RNAi} clones were induced with a 40 min heat-shock treatment at 37°C at the late second instar larval stage. *UAS-Ptpa*, *UAS-mira*^{T591A}, *UAS-mira*^{T591D} were generated in this study. The constructs were injected by Genetivision and the Institute of Biochemical and Cell Biology, China, following standard methods.

Plasmid construction

Mira full-length coding sequence was cloned into a pAHW vector (Carnegie Institution of Washington) to construct *pAHW-mira* with a 3×HA tag at the N-terminal. We generated alanine and aspartic acid point mutations using a GBclonart mutagenesis kit with *pAHW-mira* as the template.

Antibody generation

Full-length cDNA of *Ptpa* was cloned into a *pGEX-4T-1* expression vector. The GST-fusion protein was affinity purified using Sepharose-4B beads (GE Healthcare). Polyclonal anti-PTPA was raised in rabbits.

S2 cell culture, quantification and dsRNA synthesis

Drosophila S2 cells were cultured in Schneider's medium (Gibco) containing 10% fetal bovine serum (Hyclone) at 25°C. Plasmids were transfected with Effectene (Qiagen) for immunofluorescence and with X-tremeGene HP (Roche Applied Science) for 2D western blot, IP-MS and Co-IP. All dsRNA were designed using the dsCheck online tool (http://dsCheck.RNAi.jp/). Negative control (Nc) dsRNA was designed against a pBSSk (+) vector backbone. The T7 promoter sequence (TAATACGACTCACTATAGG) was added to the 5′ terminus of all primers for dsRNA generation. Primers (5′-3′) were: Nc-F, TAAATTGTAAGCGTTAATATTTTG; Nc-R, AATTCGATATCAAGCTTATCGAT; *Ptpa*-F, CGATGTCCCTTTCCTG; *Ptpa*-R, GGTAAACTGCCGGCAATTGCGAAG; CSITALICSTARTPP4CSITALICEND-F, GAGCAACTGAAGCGCTGCGA; CSITALICSTARTPP4CSITALICEND-R, CGAATCTGGTCGAGGTACTGG. All dsRNA was synthesized using the MEGAscript RNAi Kit (Ambion) and was transfected into S2 cells following the standard protocol. After dsRNA treatment for 72 h at 25°C, plasmids for *mira* variants were transfected into cells according to the manufacturer's protocol. Cells treated with Nc dsRNA served as wt controls for *Ptpa* dsRNA treatment cells.

In order to quantify Mira localization, about 100 cells that transiently expressed *pAHW-mira* and Mira variants, with or without *Ptpa* knockdown, were analyzed using Olympus imaging software FW10-ASW (3.0) to generate histograms. Pixel intensity and cytoplasm were directly compared. Cells in which the ratio of cortex to cytoplasm staining was less than 1.0 were scored as cytoplasmic localization. Cells with a ratio between 1.0 and 1.9 were scored as cytoplasmic and cortical localization. Finally, cells with a ratio of 2 and greater were scored as cortical localization.

Immunofluorescence staining and antibodies

The larval brain and S2 cell immunofluorescence staining protocols were conducted as previously described (Azam et al., 2007; Sousa-Nunes et al., 2009). The following primary antibodies were used: rabbit anti-PTPA, 1:1000 (this study); mouse anti-Mira, 1:50 (F. Matsuzaki, CDB, RIKEN, Kobe, Japan); rat anti-Brat, 1:100 (J. Knoblich, IMBA, Vienna, Austria); mouse anti-Pros, 1:5 (Developmental Studies Hybridoma Bank); rabbit anti-PKCζ C20, 1:1000 (Santa Cruz Biotechnology, sc-216); guinea pig anti-Numb, 1:1000 (J. Skeath, University of Washington, Seattle, WA, USA); rat anti-Flfl, 1:1000 (R. Sousa-Nunes, KCL, London, UK); mouse anti-Myc 9E10, 1:500 (Sigma-Aldrich, 05-419); mouse anti-HA 12CA5, 1:1000 (Roche Applied Science, 1583816); goat anti-PPX (PP4-19C), 1:500 (Santa Cruz Biotechnology, sc-6118); rabbit anti PPP4C (PP4-19C), 1:500 (Thermo Science, PA528786); rabbit anti-GFP, 1:1000 (Invitrogen, A6455); mouse anti-β-tubulin 1:100 (Developmental Studies Hybridoma Bank). All commercial secondary antibodies used were from the Jackson Laboratory. DNA was stained with TO-PRO3 iodide (Invitrogen) at 1:5000. Images were obtained using a Zeiss LSM 510 upright and Olympus FV1000 confocal microscope using a 40×1.30 NA oil-immersion objective and were processed with Adobe Photoshop (version CS6) and ImageJ.

Western blot

For western blots, S2 cells and L3 brains were lysed in RIPA lysis buffer [50 mM Tris-HCl pH 8.0, 150 mM NaCl, 1% (v/v) SDS, 0.5% (w/v) sodium deoxycholate, complete protease inhibitor cocktail and PhosStop phosphatase inhibitor cocktail]. For 2D western blots, S2 cells and L3 brain extracts were made with urea lysis buffer (8 M urea, 4% CHAPS, 2% IPG Buffer, 40 mM DTT, complete protease inhibitor cocktail, PhosStop phosphatase inhibitor cocktail). Total protein (~50-100 µg) was loaded for each experiment and isoelectric focusing (IEF) was performed with an IPGphor (GE Healthcare). Anti-β-tubulin signals were used to align various samples to compare the migration pattern of Mira and its variants.

Immunoprecipitation-mass spectrometry and co-immunoprecipitation

S2 cells were lysed in modified RIPA lysis buffer [50 mM Tris-HCl pH 8.0, 150 mM NaCl, 1% (v/v) IGRPA CA-630, 0.5% (w/v) sodium deoxycholate, complete protease inhibitor cocktail, PhosStop phosphatase inhibitor cocktail]. HA-tagged recombinant proteins were captured with ~5 µg rabbit anti-HA antibody (Abcam, ab9110) and Protein A-agarose beads (Roche Applied Science) according to the manufacturer's protocol. The supernatants of immunoprecipitated beads were separated on 8% SDS-PAGE following standard protocol. For detecting ectopically expressed Mira, gels were stained with Coomassie Brilliant Blue R-250 and the corresponding bands were excised. Phosphorylation sites were identified using a LTQ-Orbitrap MS at the Institute of Physics, Chinese Academy of Sciences, China.

For the Co-IP experiment, the S2 cell lysate was immunoprecipitated with ~5 µg goat anti-PPX (PP4-19C) antibody (Santa Cruz Biotechnology, sc-6188) or goat IgG with Protein A-agarose beads. The supernatants eluted from immunoprecipitated beads were loaded for western blotting following standard protocols.

Live imaging

His2av::mRFP,wor-gal4;UAS-mira::3GFP (used as wt control) and *His2av::mRFP, wor-gal4, Ptpa; UAS-mira::3GFP* (*Ptpa*) early L3 brains were dissected in Schneider's medium and mounted with fat bodies in a FluoroDish culture dish using a standard protocol (Cabernard and Doe, 2013). Images were acquired using an Olympus FV1000 with a 30×1.05 NA oil-immersion objective (zoom 2.5), at an interval of 75 s, and processed with ImageJ, Adobe Photoshop and Illustrator.

Acknowledgements

We thank William Chia and Hongyan Wang for sharing unpublished data and mutant lines; J. Knoblich, F. Matsuzaki, C. Petritsch, K. Prehoda, the Vienna *Drosophila* RNAi Center, and the Bloomington Stock Center for fly stocks and reagents.

Competing interests

The authors declare no competing or financial interests.

Author contributions

Y.C. and X.Y. conceived and designed the research. W.G.S. performed EMS mutagenesis and established the mutant stock. Z.H. initiated the project and characterized the mutants. F.Z. identified the T591 phosphorylation status and its link to Mira localization and the PP4 function. F.C. did the PP4 MARCM experiment. H.B. performed the live imaging. H.W., Y.X. and W.G. supervised students and provided valuable input for the project. P.C.C. and Y.Y. helped to analyze *mira*^{T591A} and *mira*^{T591D} transgene expression. Z.-X.H., F.Z., Y.C. and X.Y. wrote the manuscript. All authors contributed to data interpretation.

Funding

Z.-X.H. was supported by a research fellowship from the Department of Anatomy, Yong Loo Lin School of Medicine, NUS, and bridging scholarships from IMCB, ASTAR, and TLL and Singapore Millennium Foundation. H.W., Y.Y., P.C.C. and Y.C. were supported by TLL and Singapore Millennium Foundation. F.Z., H.B., F.C., Y.X., W.G. and X.Y. were supported by grants [2013CB945600 and 2012CB966800] from the National Basic Research Program of China.

Development (2016) 143, 35-44 doi:10.1242/dev.127233

Supplementary information

Supplementary information available online at
http://dev.biologists.org/lookup/suppl/doi:10.1242/dev.127233/-/DC1

References

Atwood, S. X. and Prehoda, K. E. (2009). aPKC phosphorylates Miranda to polarize fate determinants during neuroblast asymmetric cell division. *Curr. Biol.* **19**, 723-729.

Azam, S., Drobetsky, E. and Ramotar, D. (2007). Overexpression of the cis/trans isomerase PTPA triggers caspase 3-dependent apoptosis. *Apoptosis* **12**, 1243-1255.

Bello, B., Reichert, H. and Hirth, F. (2006). The brain tumor gene negatively regulates neural progenitor cell proliferation in the larval central brain of Drosophila. *Development* **133**, 2639-2648.

Betschinger, J., Mechtler, K. and Knoblich, J. A. (2003). The Par complex directs asymmetric cell division by phosphorylating the cytoskeletal protein Lgl. *Nature* **422**, 326-330.

Betschinger, J., Mechtler, K. and Knoblich, J. A. (2006). Asymmetric segregation of the tumor suppressor brat regulates self-renewal in Drosophila neural stem cells. *Cell* **124**, 1241-1253.

Cabernard, C. and Doe, C. Q. (2013). Live imaging of neuroblast lineages within intact larval brains in Drosophila. *Cold Spring Harb. Protoc.* **2013**, 970-977.

Cayla, X., Goris, J., Hermann, J., Hendrix, P., Ozon, R. and Merlevede, W. (1990). Isolation and characterization of a tyrosyl phosphatase activator from rabbit skeletal muscle and *Xenopus laevis* oocytes. *Biochemistry* **29**, 658-667.

Chabu, C. and Doe, C. Q. (2009). Twins/PP2A regulates aPKC to control neuroblast cell polarity and self-renewal. *Dev. Biol.* **330**, 399-405.

Chai, P. C., Liu, Z., Chia, W. and Cai, Y. (2013). Hedgehog signaling acts with the temporal cascade to promote neuroblast cell cycle exit. *PLoS Biol.* **11**, e1001494.

Chao, Y., Xing, Y., Chen, Y., Xu, Y., Lin, Z., Li, Z., Jeffrey, P. D., Stock, J. B. and Shi, Y. (2006). Structure and mechanism of the phosphotyrosyl phosphatase activator. *Mol. Cell* **23**, 535-546.

Doe, C. Q., Chu-LaGraff, Q., Wright, D. M. and Scott, M. P. (1991). The prospero gene specifies cell fates in the Drosophila central nervous system. *Cell* **65**, 451-464.

Erben, V., Waldhuber, M., Langer, D., Fetka, I., Jansen, R. P. and Petritsch, C. (2008). Asymmetric localization of the adaptor protein Miranda in neuroblasts is achieved by diffusion and sequential interaction of Myosin II and VI. *J. Cell Sci.* **121**, 1403-1414.

Fellner, T., Lackner, D., Hombauer, H., Piribauer, P., Mudrak, I., Zaragoza, K., Juno, C. and Ogris, E. (2003). A novel and essential mechanism determining specificity and activity of protein phosphatase 2A (PP2A) in vivo. *Genes Dev.* **17**, 2138-2150.

Fuerstenberg, S., Peng, C.-Y., Alvarez-Ortiz, P., Hor, T. and Doe, C. Q. (1998). Identification of Miranda protein domains regulating asymmetric cortical localization, cargo binding, and cortical release. *Mol. Cell. Neurosci.* **12**, 325-339.

Ikeshima-Kataoka, H., Skeath, J. B., Nabeshima, Y.-I., Doe, C. Q. and Matsuzaki, F. (1997). Miranda directs Prospero to a daughter cell during Drosophila asymmetric divisions. *Nature* **390**, 625-629.

Inaba, M. and Yamashita, Y. M. (2012). Asymmetric stem cell division: precision for robustness. *Cell Stem Cell* **11**, 461-469.

Krahn, M. P., Egger-Adam, D. and Wodarz, A. (2009). PP2A antagonizes phosphorylation of Bazooka by PAR-1 to control apical-basal polarity in dividing embryonic neuroblasts. *Dev. Cell* **16**, 901-908.

Kraut, R., Chia, W., Jan, L. Y., Jan, Y. N. and Knoblich, J. A. (1996). Role of Inscuteable in orienting asymmetric cell divisions in Drosophila. *Nature* **383**, 50-55.

Lee, C.-Y., Wilkinson, B. D., Siegrist, S. E., Wharton, R. P. and Doe, C. Q. (2006). Brat is a Miranda cargo protein that promotes neuronal differentiation and inhibits neuroblast self-renewal. *Dev. Cell* **10**, 441-449.

Lu, B., Rothenberg, M., Jan, L. Y. and Jan, Y. N. (1998). Partner of Numb colocalizes with Numb during mitosis and directs Numb asymmetric localization in Drosophila neural and muscle progenitors. *Cell* **95**, 225-235.

Matsuzaki, F., Ohshiro, T., Ikeshima-Kataoka, H. and Izumi, H. (1998). Miranda localizes Staufen and Prospero asymmetrically in mitotic neuroblasts and epithelial cells in early Drosophila embryogenesis. *Development* **125**, 4089-4098.

Neumüller, R. A. and Knoblich, J. A. (2009). Dividing cellular asymmetry: asymmetric cell division and its implications for stem cells and cancer. *Genes Dev.* **23**, 2675-2699.

Ogawa, H., Ohta, N., Moon, W. and Matsuzaki, F. (2009). Protein phosphatase 2A negatively regulates aPKC signaling by modulating phosphorylation of Par-6 in Drosophila neuroblast asymmetric divisions. *J. Cell Sci.* **122**, 3242-3249.

Petronczki, M. and Knoblich, J. A. (2001). DmPAR-6 directs epithelial polarity and asymmetric cell division of neuroblasts in Drosophila. *Nat. Cell Biol.* **3**, 43-49.

Rhyu, M. S., Jan, L. Y. and Jan, Y. N. (1994). Asymmetric distribution of numb protein during division of the sensory organ precursor cell confers distinct fates to daughter cells. *Cell* **76**, 477-491.

Schober, M., Schaefer, M. and Knoblich, J. (1999). Bazooka recruits Inscuteable to orient asymmetric cell divisions in Drosophila neuroblasts. *Nature* **402**, 548-551.

Schuldt, A. J., Adams, J. H. J., Davidson, C. M., Micklem, D. R., Haseloff, J., St Johnston, D. and Brand, A. H. (1998). Miranda mediates asymmetric protein and RNA localization in the developing nervous system. *Genes Dev.* **12**, 1847-1857.

Shen, C.-P., Jan, L. Y. and Jan, Y. N. (1997). Miranda is required for the asymmetric localization of Prospero during mitosis in Drosophila. *Cell* **90**, 449-458.

Shen, C.-P., Knoblich, J. A., Chan, Y.-M., Jiang, M.-M., Jan, L. Y. and Jan, Y. N. (1998). Miranda as a multidomain adapter linking apically localized Inscuteable and basally localized Staufen and Prospero during asymmetric cell division in Drosophila. *Genes Dev.* **12**, 1837-1846.

Smith, C. A., Lau, K. M., Rahmani, Z., Dho, S. E., Brothers, G., She, Y. M., Berry, D. M., Bonneil, E., Thibault, P., Schweisguth, F. et al. (2007). aPKC-mediated phosphorylation regulates asymmetric membrane localization of the cell fate determinant Numb. *EMBO J.* **26**, 468-480.

Sousa-Nunes, R. and Somers, W. G. (2010). Phosphorylation and dephosphorylation events allow for rapid segregation of fate determinants during Drosophila neuroblast asymmetric divisions. *Commun. Integr. Biol.* **3**, 46-49.

Sousa-Nunes, R., Chia, W. and Somers, W. G. (2009). Protein phosphatase 4 mediates localization of the Miranda complex during Drosophila neuroblast asymmetric divisions. *Genes Dev.* **23**, 359-372.

Vaessin, H., Grell, E., Wolff, E., Bier, E., Jan, L. Y. and Jan, Y. N. (1991). prospero is expressed in neuronal precursors and encodes a nuclear protein that is involved in the control of axonal outgrowth in Drosophila. *Cell* **67**, 941-953.

Van Hoof, C., Martens, E., Longin, S., Jordens, J., Stevens, I., Janssens, V. and Goris, J. (2005). Specific interactions of PP2A and PP2A-like phosphatases with the yeast PTPA homologues, Ypa1 and Ypa2. *Biochem. J.* **386**, 93-102.

Wang, H., Somers, G. W., Bashirullah, A., Heberlein, U., Yu, F. and Chia, W. (2006). Aurora-A acts as a tumor suppressor and regulates self-renewal of Drosophila neuroblasts. *Genes Dev.* **20**, 3453-3463.

Wang, H. Y., Ouyang, Y. S., Somers, W. G., Chia, W. and Lu, B. W. (2007). Polo inhibits progenitor self-renewal and regulates Numb asymmetry by phosphorylating Pon. *Nature* **449**, 96-100.

Wang, C., Chang, K. C., Somers, G., Virshup, D., Ang, B. T., Tang, C., Yu, F. and Wang, H. (2009). Protein phosphatase 2A regulates self-renewal of Drosophila neural stem cells. *Development* **136**, 2287-2296.

Wirtz-Peitz, F., Nishimura, T. and Knoblich, J. A. (2008). Linking cell cycle to asymmetric division: Aurora-A phosphorylates the Par complex to regulate Numb localization. *Cell* **135**, 161-173.

Wodarz, A., Ramrath, A., Kuchinke, U. and Knust, E. (1999). Bazooka provides an apical cue for Inscuteable localization in Drosophila neuroblasts. *Nature* **402**, 544-547.

Wodarz, A., Ramrath, A., Grimm, A. and Knust, E. (2000). Drosophila atypical protein kinase C associates with Bazooka and controls polarity of epithelia and neuroblasts. *J. Cell Biol.* **150**, 1361-1374.

Yousef, M. S., Kamikubo, H., Kataoka, M., Kato, R. and Wakatsuki, S. (2008). Miranda cargo-binding domain forms an elongated coiled-coil homodimer in solution: implications for asymmetric cell division in Drosophila. *Protein Sci.* **17**, 908-917.

Yu, F., Morin, X., Cai, Y., Yang, X. and Chia, W. (2000). Analysis of partner of Inscuteable, a novel player of Drosophila asymmetric divisions, reveals two distinct steps in Inscuteable apical localization. *Cell* **100**, 399-409.

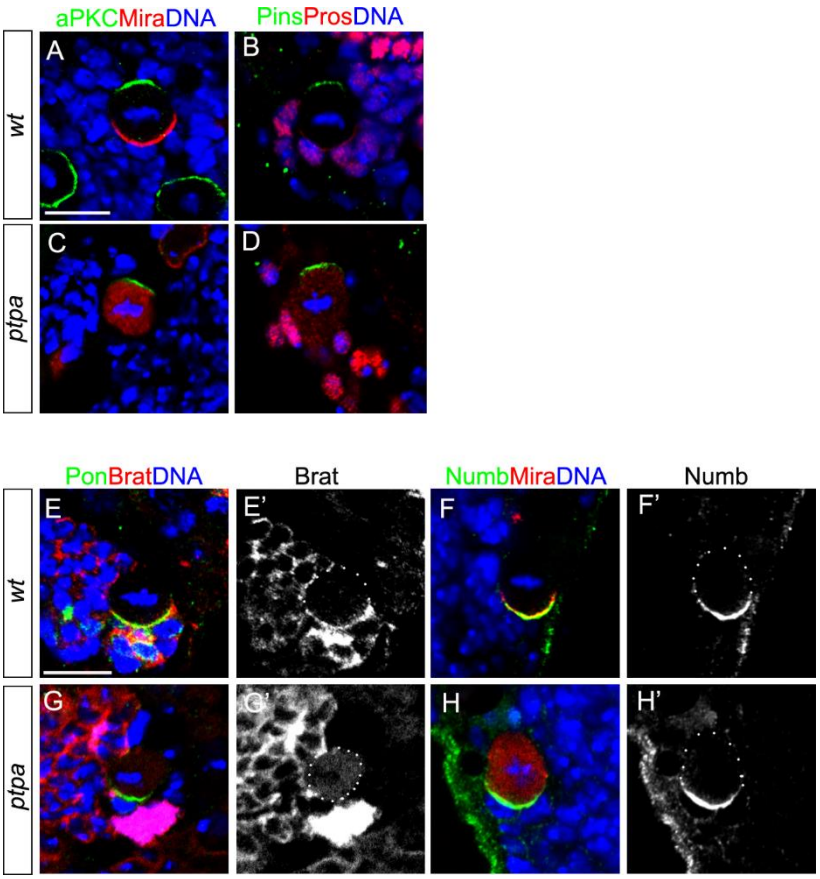

Fig. S1. Disruption of *ptpa* causes a mislocalization of the Mira complex during metaphase in L3 larval brain NBs. (A-D), aPKC and Pins apical localization remains undisturbed in the *ptpa* mutant NBs (C, D) as compared with *wt* (A, B), whereas Mira (C) and Pros (D) exhibit cytoplasmic localization in *ptpa* mutant NBs. (E-H), Brat and Mira form a basal crescent in *wt* NBs (E, F) but are mislocalized in *ptpa* mutant NBs (G, H). Pon and Numb localize to the basal cortex in both *wt* (E, F) and *ptpa* mutant (G, H) NBs. NBs are outlined with dots. Scale bar is 10µm.

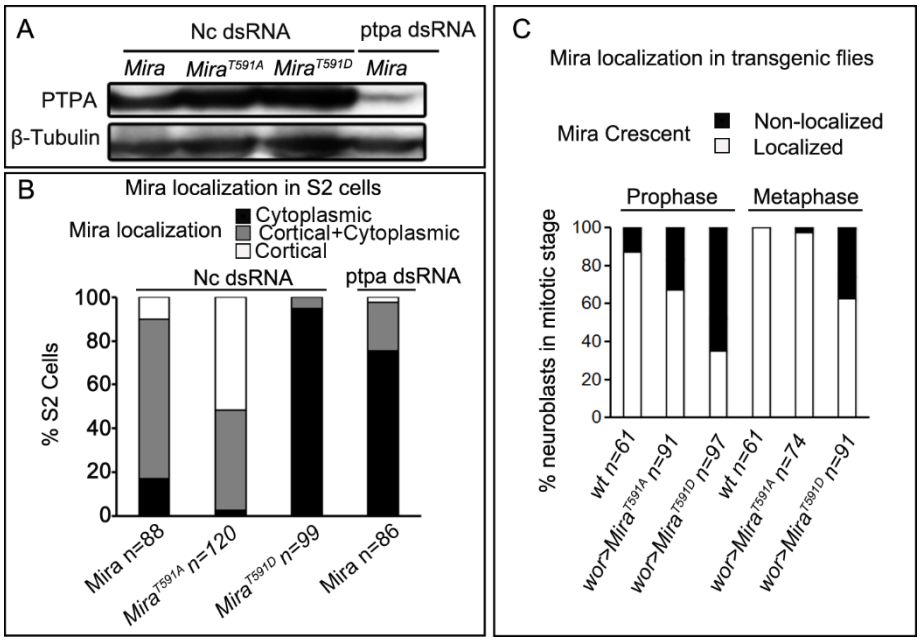

Fig. S2. Phosphorylation status of T591 residue affects Mira localization. (A), PTPA level is significantly decreased in *ptpa* dsRNA treated S2 cells (comparing lane 4 with other lanes). (B), Quantification of Mira and its variants' localization in S2 cells. (C), Quantification of Mira and its variants' localization in prophase and metaphase NBs of L3 larval brains.

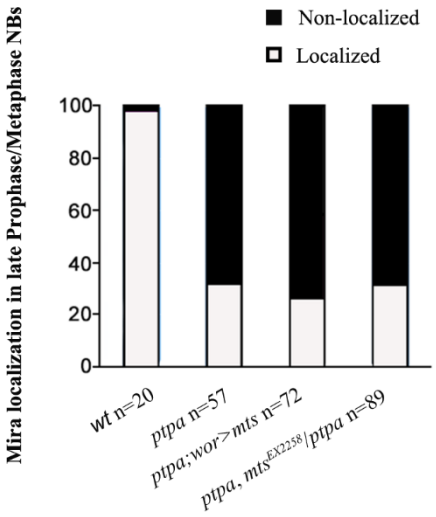

Fig. S3. PTPA does not act with Mts to mediate Mira localization. Quantification of Mira localization in prometaphase/metaphase NBs of L3 larval brains in various genetic backgrounds and with different levels of Mts.

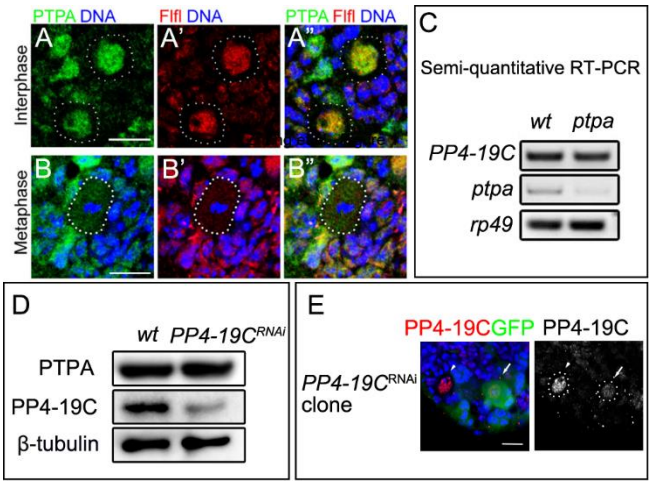

Fig. S4. PTPA and PP4 act in the same genetic pathway. (A-B), In *wt* NBs, PTPA (green) and Flfl (red) co-localize in NBs during interphase and metaphase. (C), Semi-quantitative RT-PCR result reveals that *PP4-19C* transcript levels were not affected in the *ptpa* mutant L3 larval brain. (D, E), *PP4-19C* RNAi transgene effectively reduces PP4-19C protein levels in *wt* brains (driven by *wor-gal4* driver) as indicated by the Western Blotting analysis (D), as well as in individual NBs (E, NB expressing *PP4-19C* RNAi transgene is indicated by arrow, compared with *wt* NB marked by arrowhead). Scale bar is 10μm.

Movie 1. A *wt* NB showing Mira's sequential localization during asymmetric cell division. Genotype: *Histone::mRFP*, *wor-gal4*; *Mira::3GFP*.

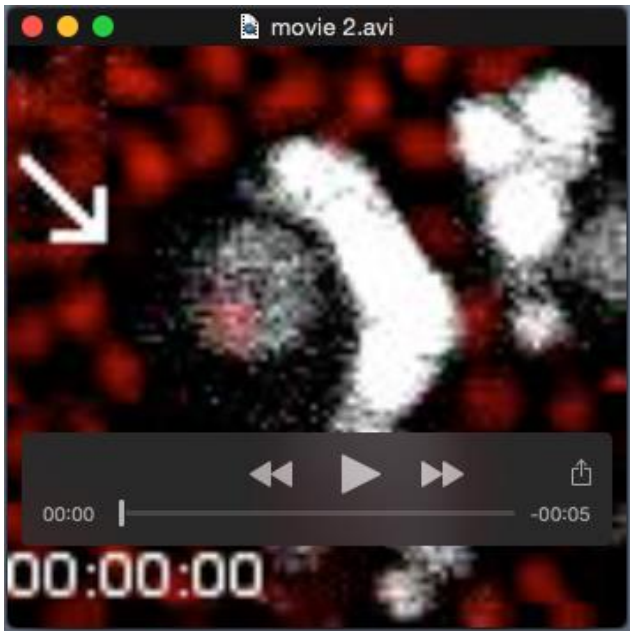

Movie 2. A *ptpa* mutant NB showing Mira localization during asymmetric cell division. Genotype: *Histone::mRFP*, *wor-gal4*, *ptpa*; *Mira::3GFP*.